New Zealand Journal of Geology and Geophysics, 1997, Vol. 40: 43–52
0028–8306/97/4001—0043 $2.50/0

Fluid inclusion evidence for geothermal structure beneath the Southern Alps, New Zealand

D. CRAW
Geology Department
University of Otago
P.O. Box 56
Dunedin, New Zealand

Abstract Fissure veins containing adularia, bladed calcite, quartz, and chlorite occur in fractures in schist immediately west of the mountain crest in the Southern Alps, an active collisional mountain range. The vein minerals contain primary fluid inclusions which homogenise between 240 and 260°C. The fluids have low dissolved salt content (<2 wt% NaCl equivalent) and low CO_2 content (<1 wt%). Fluid inclusions in adularia show physical (co-existing liquid and vapour) and chemical (variable CO_2 contents) evidence for boiling during entrapment. The mineral assemblage is similar to that seen in boiling zones of modern geothermal systems. Boiling occurred at 500 ± 150 m below topographic surface, or c. 1 km above sea level, and fluid temperature was higher than rock temperature. In contrast, fluids trapped in the same rock sequence at 300–350°C at 6–10 km under lithostatic and hydrostatic fluid pressure were approximately the same temperature as host rock and define part of a conductive thermal anomaly. The boiling zone developed due to topography-driven two-dimensional circulation of meteoric water into the uplift-induced conductive anomaly, followed by rapid buoyant rise of heated and partially isotopically exchanged water to shallow levels under hydrostatic fluid pressure.

Farther west, near the Alpine Fault, the conductive thermal anomaly has resulted in fluid and rock temperatures of 300–350°C at <5–8 km under lithostatic and hydrostatic fluid pressure. The fluid is mainly meteoric in origin, but has partially exchanged isotopically with the host rock. Minor buoyant rise of fluid has resulted in penetration of hot (200°C) fluid into relatively cool rock at shallow levels (<2 km). Hot springs emanate from the surface above this portion of the hydrothermal system, but these springs are fed by topographically driven meteoric water, which penetrates to only shallow levels in the crust and is isotopically distinct from the deeper fluids.

Keywords fluid inclusions; boiling; immiscibility; fluid pressure; heat flow; Southern Alps; tectonics; mountains

INTRODUCTION

Warm springs (typically <60°C) occur in many active deformational zones (Barnes 1970; Barnes et al. 1978; Bhattarai 1980) despite the absence of the volcanic activity usually assumed to drive such systems (Henley 1985). These springs are the only surface expressions of locally anomalous conductive heat flow driven by tectonic uplift (Allis et al. 1979; Koons 1987; Allis & Shi 1995). However, the spring feeder systems are subject to the vagaries of near-surface cold-groundwater flow, and may be obscured by such flow. Hence, some mountain belts, or portions of mountain belts, may show no surface expression of high heat flow. Other evidence of locally anomalous heat flow in collisional belts has been obtained from fluid-inclusion studies of veins formed during uplift (Holm et al. 1989; Craw et al. 1994a) and from thermochronological systems (Kamp et al. 1989; Allis & Shi 1995). These studies suggest that anomalous thermal gradients and hot fluid flow are an essential part of collisional zone processes.

The two-dimensional shape of these tectonically induced thermal anomalies is poorly known, and that knowledge is limited to thermal models calculated for some generalised tectonic conditions (Koons 1987; Craw et al. 1994a; Allis & Shi 1995). These models have very limited geological constraints provided by mainly one-dimensional fluid-inclusion and thermochronological data. The models focus on crustal-scale conductive heat flow associated with advection of hot rocks from depth at rates faster than the rocks can cool. At a more local scale, however, mobility of hot fluid can have a dramatic effect on small scale features such as rock fractures and the veins which they host. This small scale fluid mobility is the topic of the present study.

This paper attempts to use fluid inclusions and fluid geochemistry to provide some constraints on the two-dimensional geometry of the thermal anomaly beneath the western part of the central Southern Alps of New Zealand, and to examine evidence for hot fluid mobility. Thus, the paper is presented in two principal parts. The first part presents detailed evidence for hot fluid circulation and migration to very shallow levels at high altitudes, even though there is no surface manifestation of this hot fluid flow. The second part attempts to provide some fixed temperature-depth points to constrain the geometry of the thermal anomaly in two dimensions. All the data are then combined to provide a speculative two-dimensional section through the geothermal system.

GEOLOGICAL SETTING

The Southern Alps is an actively rising mountain belt being formed by continental collision between the Pacific and Australian plates (Fig. 1). The plate boundary, the Alpine Fault (Fig. 1), is an oblique-slip fault which currently has c. 8 mm/yr vertical motion (Bull & Cooper 1986; Simpson et al. 1994), east side up. Immediately east of the Alpine Fault, mid-crustal amphibolite facies rocks are being exhumed due to this uplift (Cooper 1980), as erosion keeps pace with uplift (Koons 1989). Farther east, uplift rates are

G96005
Received 19 February 1996; accepted 9 August 1996

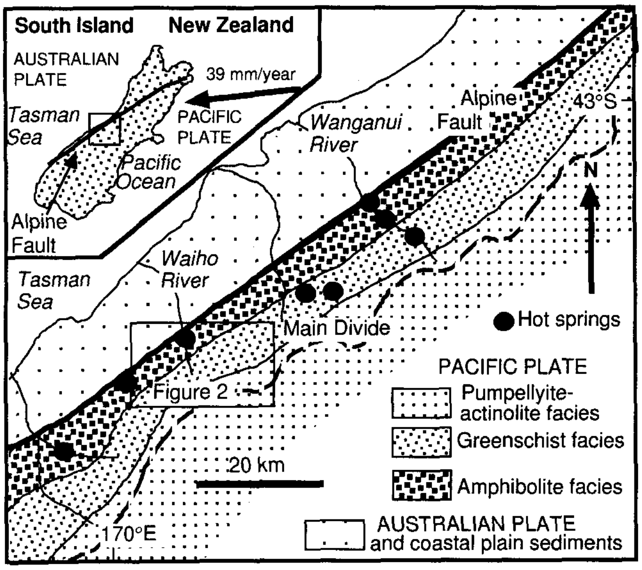

Fig. 1 Location map of the Southern Alps active mountain belt southwest of the Alpine Fault plate boundary.

lower, and erosion rates are lower as well (Koons 1989). Greenschist facies rocks have been exhumed on the western side of the mountains (Fig. 1), and the main mountain chain is predominantly prehnite-pumpellyite and pumpellyite-actinolite facies rocks, which have experienced little more uplift than the present relief indicates (Koons 1989). Hence, the zonation in metamorphic grade east of the Alpine Fault approximates an upturned crustal section (Wellman 1979). The present paper focusses on the greenschist facies and amphibolite facies rocks west of the Main Divide, and compares the hydrothermal systems in these two adjacent but different parts of the mountain belt.

HYDROTHERMAL SYSTEM

The high relief, coupled with high rainfall on the western slopes of the mountains, has caused topography-driven meteoric water penetration into the highly fractured metamorphic rocks (Koons & Craw 1991). Rapid uplift adjacent to the Alpine Fault is occurring faster than the rocks can cool, and a pronounced conductive thermal anomaly has formed in the shallow crust up to c. 15 km east of the fault (Fig. 1) (Koons 1987; Allis & Shi 1995). This thermal anomaly encourages crustal fluid circulation (Koons & Craw 1991). Fluids of probable metamorphic origin are released from the metamorphic rocks during uplift, and contribute to the fluid budget (Craw & Koons 1989; Koons & Craw 1991; Craw & Norris 1993). Shallow-circulating meteoric fluids emanate as warm springs locally (Fig. 1). Allis & Shi (1995) estimated that the hot spring systems carry <10% of the total heat flux and are controlled by limited permeability in the host schist basement.

Most previous work on the fluid circulation system has been concentrated on the central Southern Alps, where uplift rates are highest, and has focussed on the amphibolite facies rocks near the Alpine Fault (Fig. 2). Several generations of veins fill fractures in the rocks, indicating fluid activity from

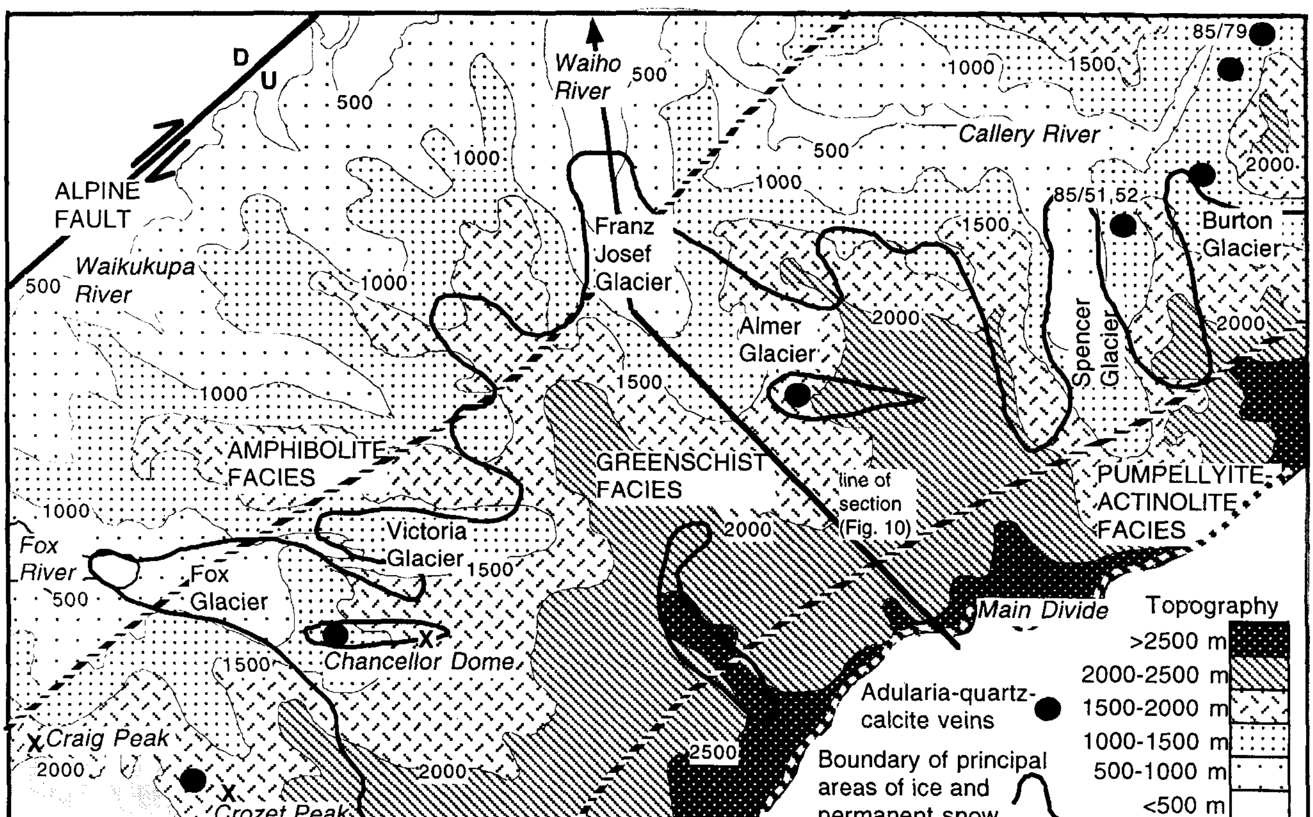

Fig. 2 Topographic map of the western central Southern Alps from the Main Divide to the Alpine Fault (see Fig. 1 for location). The principal geological features and locations for samples discussed in this study are indicated.

below the brittle-ductile transition to <1 km below the surface (Holm et al. 1989; Craw & Norris 1993; Jenkin et al. 1994). All fluids traversing the amphibolite facies rocks contain dissolved carbon dioxide, which can be up to 50 mole% of the fluid (Craw 1988; Jenkin et al. 1994).

The fluid circulation system in the greenschist facies rocks of the central Southern Alps is more poorly defined than that in the amphibolite facies rocks farther west. Vein systems have been studied only in relation to the structural evolution of their host rocks, not as part of a mountain-scale hydrothermal system (Craw et al. 1987, 1994b). Observations in these preliminary studies have shown that the fluid is dominantly water, with little carbon dioxide.

TOPOGRAPHY

The western Southern Alps have over 3 km of relief between the crest of the range (Main Divide) and the coastal plain at the Alpine Fault 15 km away (Fig. 2). The range is drained by numerous closely spaced rivers, which trend approximately perpendicular to the Alpine Fault and the Main Divide (Koons 1989). These rivers are powerfully erosive in their lower reaches, and can remove bedrock as fast as it is exposed by the Alpine Fault (Koons 1989). Hence, the westernmost area, underlain by amphibolite facies rocks, consists of steep-sided ridges and deeply incised valleys. In contrast, near the Main Divide, topography is less pronounced, and there is a broad bench at c. 1500–2000 m in which there is much less difference in altitude between ridge and valley than farther west (Fig. 2). The upper reaches of the Callery valley (Fig. 2) have been cut into this bench since deglaciation began c. 15 000 years ago.

The pronounced topography in the amphibolite facies zone is important for fluid circulation and vein formation during uplift. With >1500 m of steep relief in a high rainfall area, these ridges must impose three-dimensional flow to circulating meteoric water at shallow to intermediate depths. Hot springs occur only in the valleys in this zone (Fig. 1); all springs observed on the steep slopes are cold. The numerous suites of veins in amphibolite facies rocks are found almost exclusively in valley floors. All the data on the latter stages of uplift of these rocks (e.g., Holm et al. 1989; Craw & Norris 1993; Jenkin et al. 1994) were obtained from valley floor veins in the Fox and Waiho valleys (Fig. 2). Despite extensive searching in locally excellent outcrop on ridges, no areas of widespread veining similar to valley floor systems have been found. The few late-stage veins found on ridge crests are narrow, fine grained, and yielded no useful fluid-inclusion information. A single large vein in amphibolite facies rocks on a ridge crest near Craig Peak (Fig. 2) formed near to the low-relief bench and at sufficient depth that the distinction between ridge and valley apparently did not matter (Craw et al. 1994b). Hence, upflow of hot fluid and consequent vein mineralisation in the upper few kilometres (scale of topography) is apparently focussed in the region at and below the valleys, rather than beneath the ridges.

IMMISCIBLE FLUIDS

Fluid inclusion evidence of fluid immiscibility during vein mineralisation provides estimates of temperature and fluid pressure of mineralisation, and several generations of such estimates can be used to define fluid thermal profiles in the crust during uplift (Holm et al. 1989). Fluid immiscibility is a common phenomenon in veins in the amphibolite facies rocks (Craw 1988; Holm et al. 1989; Jenkin et al. 1994). However, evidence of immiscibility is sparse in veins in greenschist facies rocks. Craw et al. (1994b) reported rare veins with immiscible CO_2-bearing water from Craig Peak (Fig. 2). Craw et al. (1987) suggested that some late-stage veins in the Callery River (Fig. 2) may have formed from boiling water, but definitive evidence for such boiling was lacking in that study. The first part of the present study attempts to examine this latter point in more detail, to demonstrate that boiling has occurred in the late history of the uplift of these rocks, and to examine the significance of such boiling in the context of the overall hydrothermal system in the western Southern Alps.

BOILING FLUIDS IN VEINS

Vein location and mineralogy

The presence of adularia has been used to suggest that boiling may have occurred in late-stage veins in the Southern Alps (Craw et al. 1987). Adularia veins are widespread in the central Southern Alps, principally in the Callery River (Craw et al. 1987) but also in the Franz and Fox Glacier areas (Lillie et al. 1957) (Fig. 2). These veins are invariably hosted by the greenschist facies belt, at an altitude of 1500–1800 m above sea level (Fig. 1, 2). At this position in the central Southern Alps, the vein occurrences of interest in this study occur in a zone with relatively little along-strike topographic relief, which forms a high-altitude bench (Fig. 2).

The veins vary widely in orientation, but are typically steeply dipping and fill fractures that cut schistosity and upright folds associated with Alpine Fault deformation (Cooper et al. 1987; Craw et al. 1994b). The fractures are narrow (<20 cm wide) and are generally traceable for <1 m. The mineralised fractures occur in swarms, particularly in more competent psammitic schist.

Adularia occurs as euhedral crystals 1–20 mm across, which protrude into open cavities in the fractures. The adularia crystals are commonly intergrown with prismatic quartz and platy calcite crystals up to 50 mm across. The platy calcite forms a delicate boxwork texture extending into open cavities. Quartz and adularia locally include calcite plates. Chlorite flakes up to 2 mm coat quartz, calcite, and adularia in many veins, and chlorite inclusions are common in all vein minerals.

Fluid inclusions

Adularia, quartz, and calcite contain numerous fluid inclusions up to 100 μm across. They are almost all liquid-dominated two-phase aqueous inclusions, and primary inclusions are most common. Secondary inclusion trails occur, but these are minor, and the inclusions are typically small (<20 μm). Rare vapour-rich inclusions are found in adularia and bladed calcite (Fig. 3), co-existing with clusters of liquid-rich inclusions. Adularia grains were crushed in oil between two glass slides (after Roedder 1984), and all vapour bubbles shrank on opening except in sample 85/79 (Callery River; Fig. 2) where bubbles expanded. The crushing observations imply negligible carbon dioxide

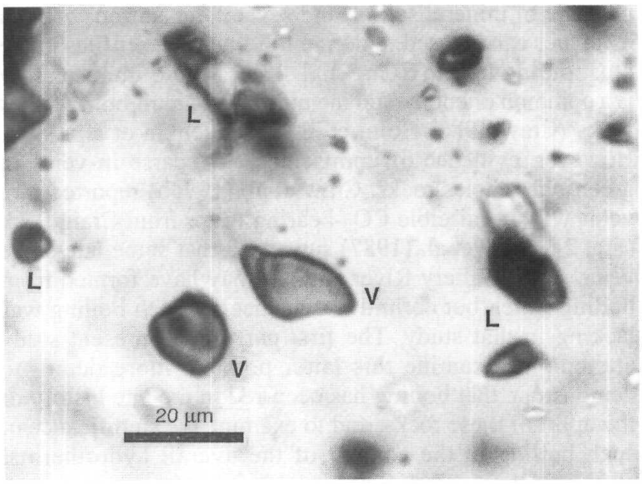

Fig. 3 Photomicrograph of co-existing liquid-rich (L) and vapour-rich (V) fluid inclusions in an adularia crystal from the Callery River (Fig. 2).

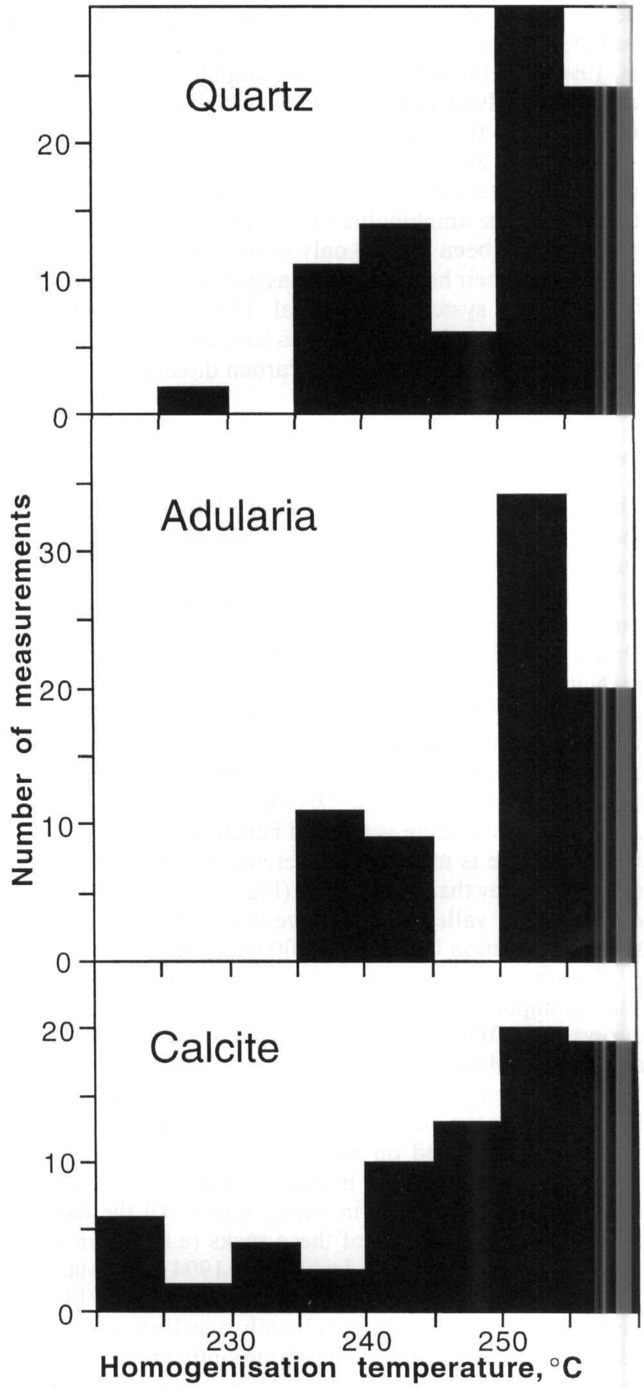

Fig. 4 Histograms of homogenisation temperatures for fluid inclusions in complexly intergrown quartz, adularia, and calcite from the Callery River, and quartz and adularia from Almer Glacier (Fig. 2).

except in sample 85/79 (Roedder 1984). Inclusions were examined microthermometrically on modified USGS heating/freezing stages in laboratories at the University of Otago (Craw 1988) and University of Calgary, and data are presented below.

Homogenisation temperatures (T_h) for primary inclusions range from 220 to 300°C for all minerals in all samples examined from adularia-bearing veins. Co-existing minerals have very similar T_h (Fig. 4). Each grain examined contains clusters of fluid inclusions in close proximity (<200 µm), which homogenise within c. 5°C of each other, and clusters elsewhere in the same grain can differ by up to 30°C (Fig. 5). The rare vapour-rich inclusions decrepitated before homogenisation above c. 280°C.

Ice-melting temperatures (T_m) are consistent within a narrow range for many samples, and generally lie between −0.8 and −1.6°C (Fig. 5, 6). Clusters of inclusions with similar homogenisation temperatures also have similar T_m, although differences in T_m between clusters are small (Fig. 5). There is no correlation between T_m and T_h (Fig. 5, 6). In particular, sample 85/79 shows a wider range of T_m than the other samples examined, and a wide range of homogenisation temperatures, but no correlation between T_m and T_h (Fig. 6). T_h for most inclusions in this sample lies in a narrow range, yet these inclusions have a wide range of T_m (Fig. 6, inset). Vapour-rich inclusions have ice-melting temperatures near 0°C, but only four inclusions were sufficiently clearly observable to obtain these data.

Secondary inclusions have consistently lower T_h than primary inclusions in the same sample (Fig. 5), although there is minor overlap in some samples. The secondary inclusions have similar T_m to the primary inclusions, but are generally at the higher end of the range for each sample (Fig. 5).

Oxygen isotope data

Oxygen isotope analyses of prismatic quartz co-existing with adularia and bladed calcite in a fissure in the Callery River (sample 85/52; Fig. 2) range from $\delta^{18}O$ = +13.1 to +9.4‰ (D. Craw & C. P. Chamberlain unpubl. data). Hence, the water had $\delta^{18}O$ = +0.4 to +4.1‰, assuming mineral growth at 250°C and the fractionations of Matsuhisa et al. (1979). Bladed calcite from the same sample has $\delta^{18}O$ = +13.0, implying water $\delta^{18}O$ = c. +5‰ at 250°C (Matsuhisa et al. 1979; Chiba et al. 1989). Calcite is not in isotopic equilibrium with the associated quartz, as $\delta^{18}O_{calcite} \geq \delta^{18}O_{quartz}$, but may have re-equilibrated with the same water that deposited the quartz, at lower temperatures (200–150°C; Chiba et al. 1989). Fluid with such low $\delta^{18}O$ is presumed to

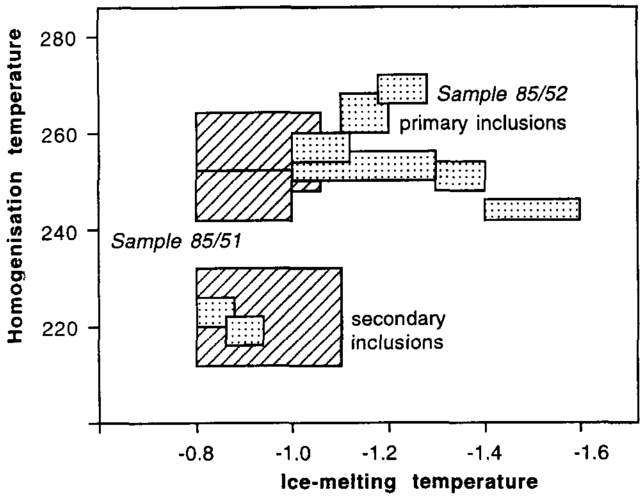

Fig. 5 Homogenisation temperatures and ice-melting temperatures for clusters of fluid inclusions from two samples of adularia from the Callery River: sample 85/51 (hatched) and sample 85/52 (stippled).

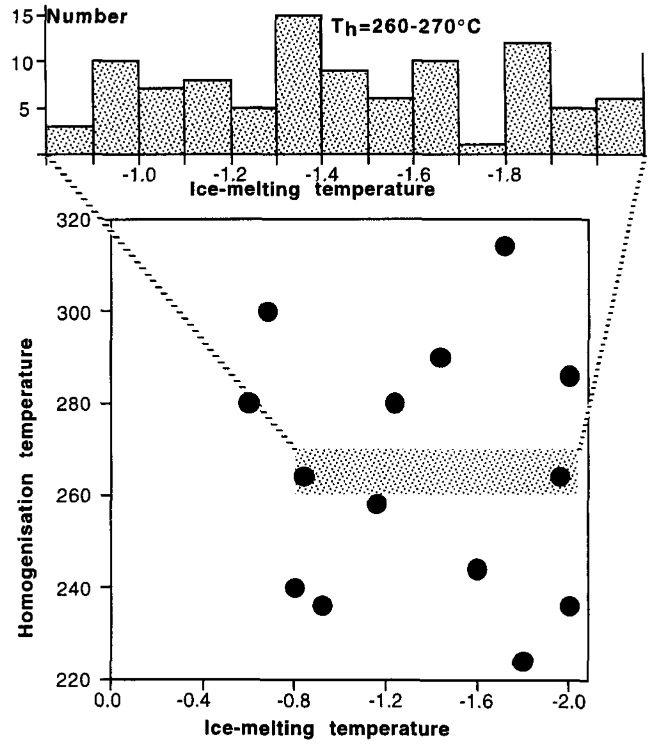

Fig. 6 Homogenisation temperatures and ice-melting temperatures for fluid inclusions from a Callery River sample (sample 85/79) of adularia. The inset is a histogram of ice-melting temperatures for the most commonly observed homogenisation temperature range.

be meteoric water which has undergone partial equilibration with the host rock (Jenkin et al. 1994).

Interpretation of fluid data

Co-existing liquid-rich and vapour-rich inclusions are good evidence for entrapment of inclusions during boiling of the fluid. Although the vapour inclusions are rare, their presence is sufficient to support boiling (Roedder 1984). The vapour-rich inclusions decrepitated at higher temperatures than homogenisation of the liquid inclusions, so the vapour-rich inclusions presumably contain some of the liquid as well as the vapour phase. No separate CO_2 phases were recognised in the vapour-rich inclusions, and freezing-point depression data preclude significant dissolved carbon dioxide. Hence, these vapour inclusions must represent boiling of a fluid which contained no carbon dioxide.

The T_m data outlined above suggest that the fluid has low and consistent salinity, not exceeding c. 2 wt% NaCl equivalent. Crushing observations (above) suggest that CO_2 will have negligible effect on salinity in most samples. Sample 85/79 inclusions do contain CO_2, and it is this sample which shows the widest range of ice-melting temperatures with little variation in T_h (Fig. 6). The variation in T_m in sample 85/79 is probably due to variable degrees of boiling-induced partition of CO_2 into the vapour phase, which is not preserved in this sample. Hence, the fluid before boiling had at least 1 wt% CO_2, equivalent to c. 1°C freezing-point depression (Hedenquist & Henley 1985), and c. 1.5 ± 0.5 wt% NaCl equivalent. After boiling, the CO_2 was lost to the vapour phase, and the same proportion of dissolved salts remained in the water. Later boiling produced salt-free water vapour in some samples.

Mineralogical effects of boiling

Boiling and loss of CO_2 has controlled mineral formation in the veins. Interpretation of above T_m data suggests that nearly all the dissolved CO_2 was lost from the main fluid. CO_2 is strongly partitioned into the vapour at the observed temperatures (Giggenbach 1980), so the observed CO_2 loss requires only c. 10% vapour phase separation (Henley 1984). This boiling-related CO_2 loss is responsible for deposition of bladed calcite (Simmons & Christenson 1994). CO_2 loss of this magnitude also causes a pH increase of about one log unit (Fournier 1985; Hedenquist & Henley 1985). This pH shift is commonly sufficient to move the fluid chemistry into the adularia stability field (Fig. 7), depending on the potassium activity in the fluid. Figure 7 is calculated assuming potassium activity is about one-tenth that of sodium, which is determined from T_m (above). Semi-quantitative microprobe examination of fluid inclusions in amphibolite facies hosted veins (Craw 1988) suggests that a Na:K ratio of about 10 is reasonable.

DEPTH OF BOILING ZONE

Fluid-inclusion homogenisation temperatures for boiling fluids represent the trapping temperature of the fluid which was on the water two-phase line during entrapment (Roedder 1984). Hence, the fluid pressure during boiling can also be determined from well-established water phase equilibria data (e.g., Fisher 1976). Homogenisation temperatures of 260 ± 20°C (above) imply fluid pressures of c. 50 ± 15 bars.

Conversion of fluid pressure estimates to depth of the boiling zone requires knowledge of the fluid pressure regime prevailing in the rock mass. Shallow-level vein mineralisation occurred primarily under hydrostatic fluid pressure in the amphibolite facies rocks immediately west of the current study (Jenkin et al. 1994). Similar hydrostatic conditions presumably prevailed in the greenschist facies

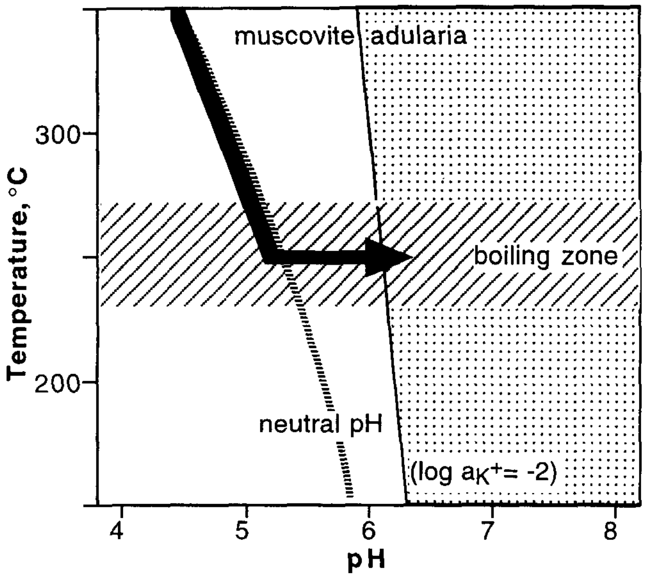

Fig. 7 Temperature-pH phase diagram for a cooling dilute fluid, showing the deduced path of the Southern Alps boiling fluid passing from the muscovite to K-feldspar stability field (see text).

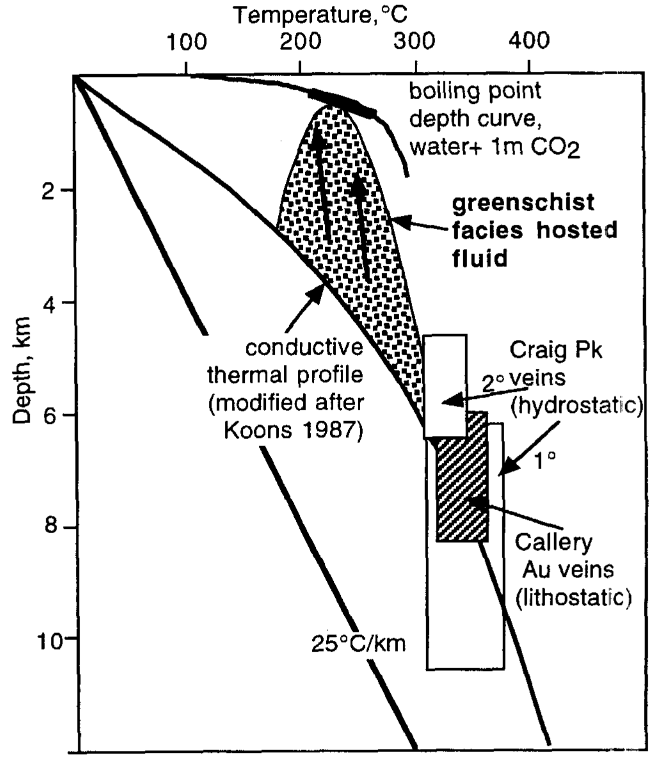

Fig. 8 Temperature-depth profile for greenschist facies schist in the western Southern Alps, assuming vertical uplift in this area. The profile is modified from the conductive model of Koons (1987) with fluid-inclusion constraints: the hatched box is for inclusions trapped under lithostatic fluid pressure, and open boxes are for hydrostatic fluid pressure, assuming an average fluid density of 0.9 g/cm^3 (see text). The heavily stippled area is the inferred zone in which fluid temperature locally departs from rock temperature near the boiling zone (see text).

host. Under hydrostatic conditions, a boiling point-depth (BPD) relationship can be calculated from fluid densities (Haas 1971), or calibrated from natural systems (Sutton & McNabb 1977). A curve drawn for a 1*M* CO_2 fluid (Sutton & McNabb 1977) is most applicable to the present study (Fig. 8), although there is little deviation from the pure water system in the temperature range of interest in this study (Henley 1985).

The BPD curve (Fig. 8) indicates that boiling in the Southern Alps occurs at c. 500 ± 150 m below the surface. This depth is only an estimate, as the BPD curve assumes that the fluid is boiling from the surface down. This is demonstrably not true in the Southern Alps as no springs are evident above the boiling zone, and the vein evidence of boiling indicates that boiling occurs in a narrow temperature (and therefore depth) interval. Hence, the density of overlying fluids is greater in the Southern Alps than for the BPD curve, and the true depth of mineralisation may be shallower than suggested by the BPD curve. Further, if hydrodynamic fluid pressure conditions prevailed, rather than hydrostatic conditions assumed for the BPD curve, even shallower boiling depths may be indicated (Henley 1985). The veins containing evidence of boiling are all found higher than c. 1400 m above sea level. The boiling zone is therefore within the observable relief, c. 1 km above sea level, beneath the high topographic bench west of the Main Divide.

FLUID TEMPERATURE-DEPTH RELATIONSHIPS

Greenschist facies hosted veins

Lithostatic veins

The conductive thermal profile for the greenschist facies rocks is undocumented in the field, but calculations based on estimated uplift rates suggest that an elevated near-surface thermal gradient results from rapid uplift (Fig. 8) (Koons 1987; Allis & Shi 1995). Fluid-inclusion and mineralogical data from late-stage veins can further constrain this profile. Gold-bearing veins formed in the greenschist facies rocks of the Callery River, near to the brittle-ductile transition. These veins locally contain the silicate assemblage quartz - muscovite - chlorite - biotite, similar to that of the host rock (Craw et al. 1987). The mineral compositions in veins and host rocks are identical, and so the vein-forming fluid and the host rock were at approximately the same temperature during mineralisation at this depth. The veins formed at c. 320–350°C and c. 1.5 kbar pressure (Craw et al. 1987). The veins are thin, discontinuous, and commonly shallow-dipping, so fluid pressure was probably lithostatic. Hence, mineralisation occurred at c. 6 km depth (Fig. 8) (Craw et al. 1987; Craw & Koons 1989).

Hydrostatic veins

Veins with open-space filling textures cut steeply across greenschist facies schistosity in the Craig Peak area (Fig. 2). The veins are up to 1 m wide and can be traced for several metres as an interconnected network. These veins are texturally and mineralogically different from the adularia-bearing veins described in the preceding sections, and contain different fluid inclusions. Hematite and chalcocite in these veins indicate oxidation relative to the surrounding rocks, which has been interpreted as being due to incursion of meteoric water (Johnstone et al. 1990). The veins have formed from water with sufficient dissolved CO_2 to become immiscible during mineralisation (Craw et al. 1994b). Mineralisation temperature and fluid pressure estimates for primary inclusions are not well defined, but are c. 350°C and 600–1000 bars. Secondary inclusions yield better data, and entrapment occurred at 310 ± 10°C and 500 ± 100 bars (Sterner & Bodnar 1991; Craw et al. 1994b). The vein mineralogy and structures are consistent with fluid pressure being hydrostatic, and so these fluids were active at c. 5–11 km depth (Fig. 8). The primary fluid overlaps the lithostatic gold-bearing veins (described above), with fluid and rock temperatures approximately the same. This zone in the crust is apparently the transition zone between predominantly lithostatic (below this level) and predominantly hydrostatic (above this level) fluid pressure regimes.

Temperature-depth profile

The Callery and Craig Peak data document with reasonable confidence a single temperature-depth "point" on the uplift path of the greenschist facies rocks: 300–350°C at c. 6–10 km. This point confirms the existence of a thermal anomaly beneath this part of the Southern Alps. The spatial geometry of the uplift path of greenschist facies rocks is unknown, and is principally a combination of northwestward motion relative to the plate boundary (Alpine Fault), and opposing southeastward overthrusting (Cox & Findlay 1995). For simplicity, I assume a net vertical uplift trajectory so that the temperature-depth uplift path represents a vertical thermal profile through the upper crust (Fig. 8).

The thermal profile constructed in Fig. 8 cannot account for the widespread shallow-level boiling fluids documented above, suggesting that fluid temperatures can deviate from rock temperatures during uplift of the greenschist facies rocks at shallower levels. The alternative, of drawing the thermal profile through the boiling fluids, results in an unrealistically high near-surface thermal gradient for which there is no evidence. The temperature-depth paths for specific aliquots of fluid are as yet unknown, but presumably lie within the stippled zone (Fig. 8). Hot fluid rising to boil at 500 m below the surface in relatively cold rocks must have risen quickly, possibly driven by seismic activity (Sibson et al. 1988; Allis & Shi 1995), and would trace an almost vertical path in temperature-depth space (Fig. 8). It is not known whether this shallow-level boiling represents rare short-lived events of fluid mobility, or some (albeit temporary) steady-state hydrothermal system. However, the widespread occurrences (Fig. 2) and large number of individual veins in a small area in, for example, the Callery valley (Fig. 2) suggest that this fluid flow was an important phenomenon in the hydrothermal history of the greenschist facies host.

Amphibolite facies hosted veins

Temperature-depth uplift path

Previous work on amphibolite facies veins has suggested that a substantial conductive thermal anomaly exists within 10 km of the Alpine Fault (Holm et al. 1989; Jenkin et al. 1994). The magnitude of this anomaly has been questioned recently by Allis & Shi (1995), and a new calibration of H_2O-CO_2 phase equilibria is available (Sterner & Bodnar 1991), so some re-evaluation of the data is required. New

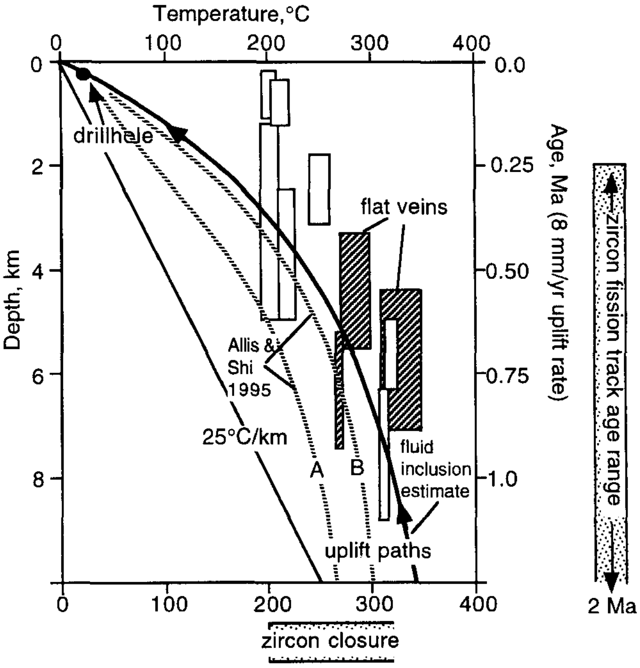

Fig. 9 Temperature-depth uplift path for amphibolite facies schist (heavy black line) based on re-evaluations of the data presented by Holm et al. (1989), and Jenkin et al. (1994) (see text). Box ornaments are as for Fig. 8; depths were calculated from hydrostatic fluid pressure assuming an average fluid density of 0.8 g/cm^3. The zircon fission track age range is from Kamp et al. (1989), and this is correlated with depth assuming constant uplift rate of 8 mm/yr (Simpson et al. 1994) over the past 1 Ma. Uplift paths derived from thermal modelling (dashed lines; Allis & Shi 1995) without (A) and with (B) frictional heating are shown for comparison.

temperature-depth estimates (with maximum depth ranges permitted by the phase equilibria) for immiscible fluids trapped in amphibolite facies veins are depicted in Fig. 9. The depths of entrapment for hydrostatic fluids are calculated assuming an average fluid density of 0.8 g/cm^3. This is a minimum plausible value, and a more realistic value of >0.9 g/cm^3 would yield >10% shallower entrapment depths. The lithostatic flat veins described by Holm et al. (1989) still yield data with the best structural control, and the inferred uplift path is forced through these data rectangles (Fig. 9). Allis & Shi (1995) suggested that these fractures may have formed lithostatically at depth and were then mineralised at shallow levels. This may be so, but mineralisation could only occur when the horizontal fractures were held open several centimetres by fluid whose pressure would therefore need to equal lithostatic pressure. Hence, even if mineralisation and fluid-inclusion entrapment postdated fracture formation, mineralisation occurred under lithostatic fluid pressure.

The thermal uplift path can also be constrained by drillhole data from the lower Waiho valley (Shi et al. 1996), drilled at the same outcrop from which some of the fluid-inclusion data were obtained. The data from this 220 m drillhole implies a thermal gradient beneath the valley of c. 95°C/km, and a terrain-corrected thermal gradient of 60 ± 15°C/km has been derived from the observational data by Allis & Shi (1995) and Shi et al. (1996) for crustal-scale modelling purposes. The uncorrected data are probably most

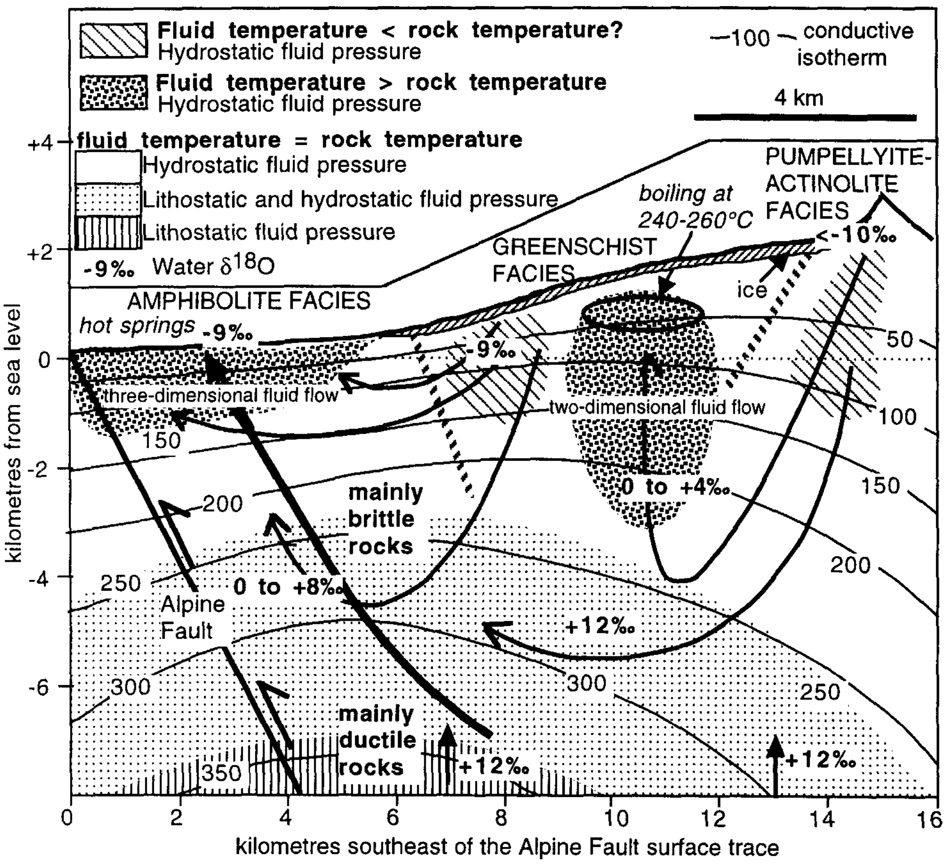

Fig. 10 Cross-section through the western central Southern Alps tectonically induced conductive thermal anomaly and associated hydrothermal system. Isotherms are modified from Koons (1987) to allow for topography and fluid inclusion derived temperature-depth profiles (Fig. 8, 9). Fluid circulation paths, and fluid temperature and pressure regimes, are speculative but are locally constrained by fluid-inclusion and isotopic data (see text).

comparable to fluid-inclusion data from rocks uplifted from shallow levels beneath the same valley floor (Fig. 9). The thermal uplift path derived from the various data (Fig. 9) is less dramatically curved than that first depicted by Holm et al. (1989) but more curved than that depicted by Allis & Shi (1995).

A further complication in the amphibolite facies rocks is the geometric relationship between the uplift path and the vertical thermal profile. The uplift path was assumed to be vertical by Holm et al. (1989), but an eastward dip subparallel to the Alpine Fault is more plausible (Fig. 10) (Allis & Shi 1995). Uncertainty about this geometry reduces the usefulness of the temperature-depth profile (Fig. 9), but the existence of a thermal anomaly is confirmed by the fluid-inclusion data.

Alternative methods of refining this anomaly are apparently of little use. Argon-based thermochronological systems are hampered by the presence of excess argon, which is known to occur in the Southern Alps (Adams 1979; Cooper et al. 1987). Hence, measured ages are maxima, and with such recent rapid uplift even small amounts of excess argon can make very large errors. Zircon thermochronology is potentially the most useful method, but the wide observed age ranges in amphibolite facies schists adjacent to the Alpine Fault (Fig. 9) (Kamp et al. 1989), combined with poorly known uplift rates, do not allow accurate depth estimates for the zircon closure temperature (c. 260 ± 60°C for rapid cooling—Yamada et al. 1995; Hurford 1986).

Shallow-level fluid temperature > rock temperature

Hot (200°C) immiscible fluids trapped at very shallow levels (Fig. 9) have a liquid water-rich end-member co-existing with inclusions dominated by CO_2 vapour (Jenkin et al. 1994). These fluids probably represent unmixing of upwardly migrating hydrostatic fluid out of thermal equilibrium with the surrounding rock (not the immediate fissure walls), similar to the boiling fluids in the greenschist facies rocks discussed above. However, this evidence of fluids with temperatures much greater than the host rock in the amphibolite facies rocks is rare and confined to microfractures in earlier formed crystals (Jenkin et al. 1994). This is distinctly different from the greenschist facies-hosted, widespread, late-stage open cavities with extensive centimetre-scale crystal growth which accompanied hot fluid migration and boiling (above).

Hot springs at sporadic locations in valleys in the amphibolite facies rocks at temperatures up to 56°C (Barnes et al. 1978) are clearly hotter than their immediate host rock and therefore indicate thermal disequilibrium during fluid migration.

CONCLUSIONS

Geothermal structure west of the Main Divide

The thermal and hydrological structures of the hydrothermal system west of the Main Divide are summarised schematically in a cross-section (Fig. 10). The section line runs along the valley floor of the Waiho River (Fig. 2) and depicts a two-dimensional approximation of the undoubtedly strongly three-dimensional meteoric fluid flow in the amphibolite facies rocks, especially at shallow levels. The conductive isotherms are modified from Koons (1987), allowing for topography and using fluid-inclusion data discussed in this study. The fluid discharge zones are defined by the areas in which fluid temperatures locally exceed rock temperatures, as indicated by shallow boiling and hot springs. Evidence for upward flow of fluid from deeper levels also occurs in the depicted discharge zones (Craw et al. 1987; Holm et al. 1989). Fluid temperature may be lower than rock temperature in the recharge zones, but no field evidence for these recharge zones has yet been found.

Oxygen isotope data for the whole hydrothermal system are also summarised in Fig. 10. These data show three main processes: metamorphic devolatilisation, meteoric incursion, and isotopic shift of meteoric water due to water-rock interaction. The latter process presumably arises when the water has a long residence time or flow path in the rock mass at temperatures sufficiently high to allow isotopic exchange. The isotopic data clearly show that there are two different levels of water flow into the amphibolite facies rocks. The shallower system involves water which recharges as meteoric waters at middle altitudes, does not exchange isotopically with the rock (Barnes et al. 1978), and discharges as hot springs (Fig. 10). The deeper waters are hotter, CO_2-bearing, and have partially exchanged isotopically with the host rock (Jenkin et al. 1994). Similar waters, with or without CO_2, have moved deep through the greenschist facies rocks (Fig. 10). The deeper, isotopically evolved waters throughout the hydrothermal system locally and rapidly penetrate to near-surface levels, where they are presumably swamped by more voluminous shallow fluids.

The section is drawn for the time of formation of the late veins from boiling fluids, as described above. This was c. 400 000 years ago, assuming 1 mm/yr uplift of the greenschist facies rocks (Craw et al. 1987; Koons 1987). A more extensive layer of ice may have coated the surface at that time, perhaps restricting supply of meteoric water beneath the ice. Hence, it is possible that the hydrothermal system depicted in the greenschist facies rocks does not exist in this form today, as deglaciation may have allowed incursion of larger amounts of cold water into what was a boiling zone. Incision by rivers such as the Callery (above) will have enhanced this effect by increasing three-dimensional relief near the Main Divide.

ACKNOWLEDGMENTS

This study was financed by the University of Otago Research Committee and the New Zealand Public Good Science Fund (Contract UO0312). Technical assistance from B. Pooley and M. Z. Stout was appreciated. Discussions, not necessarily with agreement, with C. P. Chamberlain, S. C. Cox, R. D. Johnstone, P. O. Koons, R. J. Norris, M. S. Rattenbury, and S. Simmons helped to refine the ideas expressed. P. O. Koons and R. J. Norris commented incisively on primitive versions of the manuscript, and constructive reviews by R. Allis and K. Furlong improved the clarity and substance of the paper.

REFERENCES

Adams, C. J. 1979: Age and origin of the Southern Alps. *In*: Walcott, R. I.; Cresswell, M. M. *ed*. The origin of the Southern Alps. *Royal Society of New Zealand bulletin 18*: 73–78.

Allis, R. G.; Shi, Y. 1995: New insights to temperature and pressure beneath the central Southern Alps, New Zealand. *New Zealand journal of geology and geophysics 38*: 585–592.

Allis, R. G.; Henley, R. W.; Carmen, A. F. 1979: The thermal regime beneath the Southern Alps. *In*: Walcott, R. I.; Cresswell, M. M. *ed*. The origin of the Southern Alps. *Royal Society of New Zealand bulletin 18*: 79–85.

Barnes, I. 1970: Metamorphic waters from the Pacific tectonic belt of the west coast of the United States. *Science 168*: 973–975.

Barnes, I.; Downes, C. J.; Hulston, J. A. 1978: Warm springs, South Island, New Zealand, and their potential to yield laumontite. *American journal of science 278*: 1412–1427.

Bhattarai, D. R. 1980: Some geothermal springs of Nepal. *Tectonophysics 62*: 7–11.

Bull, W. J.; Cooper, A. F. 1986: Uplifted marine terraces along the Alpine Fault, New Zealand. *Science 234*: 1225–1228.

Chiba, H.; Chacko, T.; Clayton, R. N.; Goldsmith, J. R. 1989: Oxygen isotope fractionations involving diopside, forsterite, magnetite and calcite: application to geothermometry. *Geochimica et cosmochimica acta 55*: 2867–2882.

Cooper, A. F. 1980: Retrograde alteration of chromian kyanite in metachert and amphibolite whiteschist from the Southern Alps, New Zealand, with implications for uplift on the Alpine Fault. *Contributions to mineralogy and petrology 75*: 153–164.

Cooper, A. F.; Barriero, B. A.; Kimbrough, D. L.; Mattinson, D. L. 1987: Lamprophyre dike intrusion and the age of the Alpine Fault. *Geology 15*: 941–944.

Cox, S. C.; Findlay, R. H. 1995: The Main Divide Fault Zone and its role in formation of the Southern Alps, New Zealand. *New Zealand journal of geology and geophysics 38*: 489–499.

Craw, D. 1988: Shallow level penetration of metamorphic fluids in a high uplift rate mountain belt, Southern Alps, New Zealand. *Journal of metamorphic geology 6*: 1–16.

Craw, D.; Koons, P. O. 1989: Tectonically induced hydrothermal activity and gold mineralisation adjacent to major fault zones. *Economic geology monograph 6*: 471–478.

Craw, D.; Norris, R. J. 1993: Grain boundary migration of water and carbon dioxide during uplift of garnet-zone Alpine schist, New Zealand. *Journal of metamorphic geology 11*: 371–378.

Craw, D.; Rattenbury, M. S.; Johnstone, R. D. 1987: Structural geology and vein mineralisation in the Callery River headwaters, Southern Alps, New Zealand. *New Zealand journal of geology and geophysics 30*: 273–286.

Craw, D.; Koons, P. O.; Winslow, D.; Chamberlain, C. P.; Zeitler, P. 1994a: Boiling fluids in a region of rapid uplift, Nanga Parbat Massif, Pakistan. *Earth and planetary science letters 128*: 169–182.

Craw, D.; Rattenbury, M. S.; Johnstone, R. D. 1994b: Structures within the greenschist facies Alpine Schist, central Southern Alps, New Zealand. *New Zealand journal of geology and geophysics 38*:101–112.

Fisher, J. R. 1976: The volumetric properties of H_2O: a graphical portrayal. *United States Geological Survey journal of research 4*: 189–193.

Fournier, R. O. 1985: Carbonate transport and deposition in the epithermal environment. *In*: Berger, B. R.; Bethke, P. M. *ed*. Geology and geochemistry of epithermal systems. *Reviews in economic geology 2*: 63–72.

Giggenbach, W. F. 1980: Geothermal gas equilibria. *Geochimica et cosmochimica acta 45*: 393–410.

Haas, J. L. 1971: The effect of salinity on the maximum thermal gradients of a hydrothermal system at hydrostatic pressure. *Economic geology 66*: 940–946.

Hedenquist, J. W.; Henley, R. W. 1985: The importance of CO_2 on freezing point measurements of fluid inclusions: evidence from active geothermal systems and implications for epithermal ore deposition. *Economic geology 80*: 1379–1406.

Henley, R. W. 1984: Gaseous components in geothermal processes. *In*: Henley, R. W.; Truesdell, A. H.; Barton, P. B. *ed.* Fluid-mineral equilibria in hydrothermal solutions. *Reviews in economic geology 1*: 45–56.

Henley, R. W. 1985: The geothermal framework of epithermal systems. *In*: Berger, B. R.; Bethke, P. M. *ed.* Geology and geochemistry of epithermal systems. *Reviews in economic geology 2*: 1–24.

Holm, D.; Norris, R. J.; Craw, D. 1989: Brittle and ductile deformation in a zone of rapid uplift: central Southern Alps, New Zealand. *Tectonics 8*: 153–168.

Hurford, A. J. 1986: Cooling and uplift patterns in the Lepontine Alps, south central Switzerland, and an age of vertical movement on the Insubric fault line. *Contributions to mineralogy and petrology 92*: 413–427.

Jenkin, G. R. T.; Craw, D.; Fallick, A. E. 1994: Stable isotope and fluid inclusion evidence for meteoric fluid penetration into an active mountain belt; Alpine Schist, New Zealand. *Journal of metamorphic geology 12*: 429–444.

Johnstone, R. D.; Craw, D.; Rattenbury, M. S. 1990: Southern Alps Cu-Au hydrothermal system, Westland, New Zealand. *Mineralium deposita 25*: 118–125.

Kamp, P. J. J.; Green, P. F.; White, S. H. 1989: Fission track analysis reveals character of collisional tectonics in New Zealand. *Tectonics 8*: 169–195.

Koons, P. O. 1987: Some thermal and mechanical consequences of rapid uplift: an example from the Southern Alps, New Zealand. *Earth and planetary science letters 86*: 307–319.

Koons, P. O. 1989: The topographic evolution of collisional mountain belts: a numerical look at the Southern Alps, New Zealand. *American journal of science 289*: 1041–1069.

Koons, P. O.; Craw, D. 1991: Gold mineralization as a consequence of continental collision: an example from the Southern Alps, New Zealand. *Earth and planetary science letters 103*: 1–9.

Lillie, A. R.; Gunn, B. M.; Robinson, P. 1957: Structural observations in the central alpine region of New Zealand. *Royal Society of New Zealand transactions 85*: 113–129.

Matsuhisa, Y.; Goldsmith, J. R.; Clayton, R. N. 1979: Oxygen isotopic fractionation in the system quartz - albite - anorthite - water. *Geochimica et cosmochimica acta 43*: 1131–1140.

Roedder, E. 1984: Fluid inclusions. *Mineralogical Society of America reviews in mineralogy 12.* 644 p.

Shi, Y.; Allis, R. G.; Davey, F. J. 1996: Thermal modelling of the Southern Alps. *Pure and applied geophysics 146*: 469–501.

Sibson, R. H.; Robert, F.; Poulsen, K. H. 1988: High-angle reverse faults, fluid-pressure cycling, and mesothermal gold-quartz deposits. *Geology 16*: 551–555.

Simmons, S. F.; Christenson, B. W. 1994: Origins of calcite in a boiling geothermal system. *American journal of science 294*: 361–400.

Simpson, G. D.; Cooper, A. F.; Norris, R. J. 1994: Late Quaternary evolution of the Alpine Fault Zone at Paringa, South Westland, New Zealand. *New Zealand journal of geology and geophysics 37*: 49–58.

Sterner, S. M.; Bodnar, R. J. 1991: Synthetic fluid inclusions. X. Experimental determination of P-V-T-X properties in the CO_2-H_2O system to 6 kb and 700°C. *American journal of science 291*: 1–54.

Sutton, F. M.; McNabb, A. 1977: Boiling curves at Broadlands geothermal field, New Zealand. *New Zealand journal of science 20*: 333–337.

Wellman, H. 1979: An uplift map for the South Island of New Zealand, and a model for uplift of the Souhern Alps. *In*: Walcott, R. I.; Cresswell, M. M. *ed.* The origin of the Southern Alps. *Royal Society of New Zealand bulletin 18*: 13–20.

Yamada, R.; Tagami, T.; Nishimura, S.; Ito, H. 1995: Annealing kinetics of fission tracks in zircon: an experimental study. *Chemical geology 122*: 249–258.